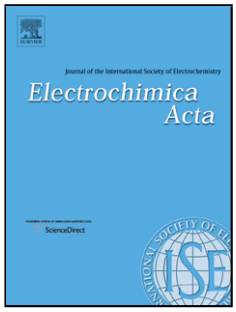

Title: Hydroxyurea electrooxidation at gold electrodes. In situ infrared spectroelectrochemical and DFT characterization of adsorbed intermediates

Authors: William Cheuquepán, José Manuel Orts, Antonio Rodes

PII: S0013-4686(17)31329-4
DOI: http://dx.doi.org/doi:10.1016/j.electacta.2017.06.091
Reference: EA 29729

To appear in: *Electrochimica Acta*

Received date: 23-3-2017
Revised date: 14-6-2017
Accepted date: 16-6-2017

Please cite this article as: William Cheuquepán, José Manuel Orts, Antonio Rodes, Hydroxyurea electrooxidation at gold electrodes.In situ infrared spectroelectrochemical and DFT characterization of adsorbed intermediates, Electrochimica Actahttp://dx.doi.org/10.1016/j.electacta.2017.06.091

Hydroxyurea electrooxidation at gold electrodes. In situ infrared spectroelectrochemical and DFT characterization of adsorbed intermediates.

William Cheuquepán[a], José Manuel Orts[&,a,b] and Antonio Rodes[a,b]

Instituto Universitario de Electroquímica[a] and Departamento de Química Física[b]

Universidad de Alicante.

Apartado 99, E-03080 Alicante, Spain.

[&]Corresponding author:

Email: jm.orts@ua.es

Phone/Fax: (+34) 965909814

Graphical abstract:

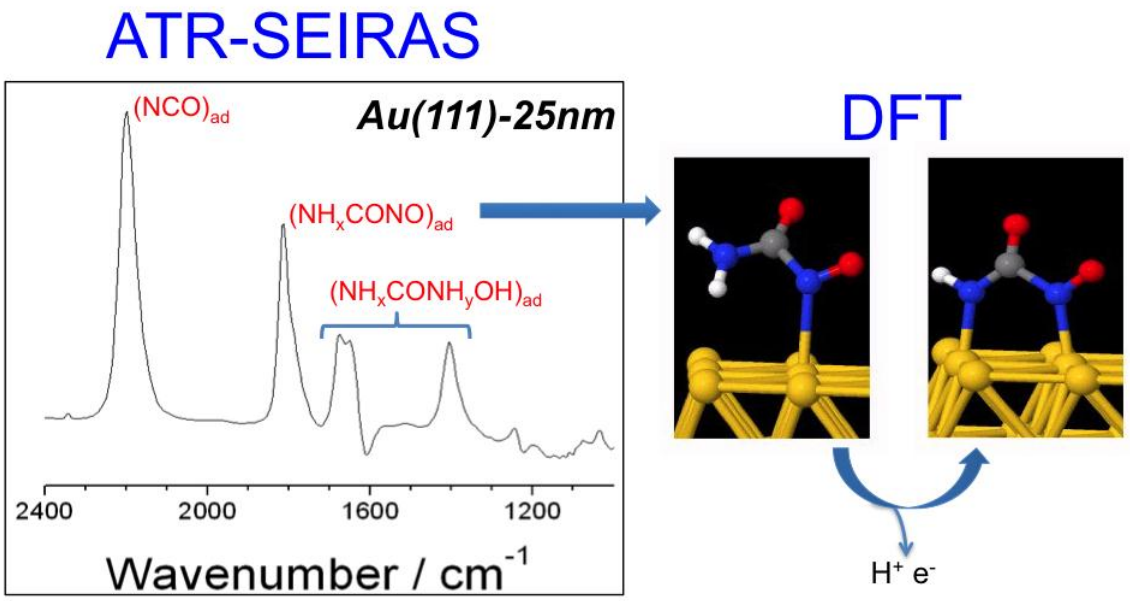

Highlights:

- Hydroxyurea oxidizes irreversibly on gold electrodes.
- CO_2, N_2O and isocyanic acid (HNCO) have been detected in solution using IRRAS.
- ATR-SEIRAS and DFT show the formation of adsorbed cyanate and nitrosoformamide.
- DFT results indicate weak adsorption of hydroxiurea at Au surfaces.

Abstract

The oxidation of hydroxyurea ($H_2NCONHOH$, HU) at Au(100), Au(111) and Au(111)-25 nm thin film electrodes is studied spectroelectrochemically in perchloric acid solutions. HU, which in agreement with DFT results interacts weakly with the gold surfaces, oxidizes irreversibly at gold electrodes irrespective of the surface orientation. The in situ external reflection spectra prove the formation of dissolved carbon dioxide and adsorbed cyanate as products of the HU electrooxidation reaction. A band at ca. 2230 cm^{-1} can be related both to dissolved isocyanic acid coming from the protonation of adsorbed cyanate or to nitrous oxide coming from the oxidation of hydroxylamine, which is formed (together with adsorbed cyanate) upon the chemical decomposition of hydroxyurea. ATR-SEIRAS experiments allow the observation of other adsorbate bands that can be tentatively ascribed to reaction intermediates that conserve the NCN skeleton and are bonded to the metal by the nitrogen atoms at near on-top positions. Bonding to the surface can be either unidentate or bidentate, involving covalent-type bonds or dative bonding – through the lone pairs of the N atoms. Some of the signals of the experimental spectra, in particular those appearing around 1800 cm^{-1} can be assigned to the CO stretch of adsorbed intermediates having a nitrosyl group formed by oxidation of the NOH moiety (namely, adsorbed nitrosoformamide or its deprotonated form). The bands observed around 1650 cm^{-1} can correspond either to the NO stretching mode of the former species or to the CO stretching modes of adspecies conserving the NOH group.

Keywords: Au(111); Au(100); gold thin film ; hydroxyurea electrooxidation; IRRAS; ATR-SEIRAS

1. Introduction.

Hydroxyurea (HU, also named hydroxycarbamide, $NH_2CONHOH$) is a simple derivative of urea that has been used as an effective treatment against sickle cell anemia and other cancers [1-4]. Several research works have been published regarding the homogeneous chemical oxidation of HU [5-9]. Under these conditions the formation of nitrosoformamide (NH_2CONO), coming from a nitroxyl radical ($NH_2CONHO\cdot$), has been proposed [5-9]. Final products reported for the oxidation of HU are carbon dioxide [5-9], ammonia [5-8], hydroxylamine [7] and nitrous oxide [5-8]. Nitrate and nitrite have also been detected in solution and considered as evidences of the formation of nitric oxide [9]. The latter species has been proposed to be at the origin of some beneficial effects of HU [1,2].

In contrast with the publication of various papers dealing with the adsorption and oxidation of urea [10-15] and some of its derivatives such as semicarbazide [16] or carbohydrazide [17], there are only a few studies regarding the electrochemical behaviour of HU. Naik et al. studied voltammetrically the electrochemical oxidation of HU at carbon electrodes [18,19] assuming the formation of nitrosoformamide as the reaction product via a two-electron oxidation reaction. Nigovic et al. studied voltammetrically the redox behavior of the Fe(III)-HU complex at a platinum electrode [20]. In a recent paper [21] , we reported for the first time the electrochemical behavior of HU at (111)-oriented gold electrodes by combining voltammetric experiments with in situ infrared experiments both under external reflection (IRRAS, InfraRed Reflection Absorption Spectroscopy) and internal reflection (ATR-SEIRAS, Attenuated Total Reflection - Surface Enhanced Infrared Reflection Absorption Spectroscopy) conditions. In this work, the formation of carbon dioxide and adsorbed cyanate as reaction products was proved, thus suggesting the existence of parallel paths regarding the fate of the carbon atom in the HU molecule. Formation of cyanate indicates the occurrence of a process that could be considered as the opposite of the synthesis of hydroxyurea from hydroxylamine and cyanate [1]. Regarding the formation of carbon dioxide, this could come from the oxidation of adsorbed cyanate [22,23] as well as from the direct oxidation of HU to hydroxylamine. The latter species would readily oxidize at gold electrodes to nitrous oxide [24]. This species could be at the origin of the band at 2231 cm^{-1} detected in the external reflection infrared spectra. Alternatively, this feature could also be related to the protonation of adsorbed cyanate to yield isocyanic acid in solution. Finally, the ATR-SEIRA spectra provided evidences for the formation at the gold electrode surface of some oxidation intermediates other that adsorbed cyanate. One of these adspecies was tentatively proposed to be adsorbed nitrosoformamide [21]. However, the assignment of such a band, as well as other bands observed in the ATR-SEIRA spectra, requires

the calculation of geometries and frequencies for the adsorbed species that could be formed upon HU reactive adsorption and electrooxidation. The aim of this work is to present the results of DFT (Density Functional Theory) calculations of the optimized geometries and harmonic vibrational frequencies of some plausible adsorbed intermediates that can be formed from HU at the Au(111) surface. On the basis of these results, we assign the adsorbate bands observed in ATR-SEIRAS experiments between 1900 and 1300 cm^{-1}. In addition, the preliminary experimental spectroelectrochemical study of the HU electrooxidation reaction is extended to a wider range of HU concentrations and to the structural aspects of this surface process by showing the results obtained with Au(100) electrodes.

2. Experimental Section

HU solutions were prepared by dissolving the corresponding amount of the solid (98% Calbiochem ® Merck Millipore) in perchloric acid solutions made from the concentrated acid (Merck Suprapur®) and ultrapure water (18.2 MΩ·cm, TOC 50 ppb max, Elga Vivendi). These solutions were deaerated with Ar (N50, Air Liquide) and blanketed with this gas during the experiments. Solutions in deuterated water were prepared with deuterium oxide (99.9 atom %D, Aldrich) which was used as received.

Clavilier's method [25,26] was employed to prepare, from a 99,9998% gold wire (Alfa-Aesar), the single crystals used as working electrodes in the electrochemical (ca. 2.0 mm in diameter) and in situ external reflection infrared spectroscopy (diameter around 4.5 mm) experiments. Prior to each experiment, these electrodes were heated in a gas-oxygen flame, cooled down in air and protected with a droplet of ultrapure water [26-28]. In the internal reflection infrared spectroscopy experiments, the working electrode was a 25 nm-thick gold thin film (Kurt J. Lesker Ltd., 99.999%) thermally evaporated on a low oxygen-content silicon prism (Pastec Ltd, Japan) . Film deposition was carried out in the vacuum chamber of a PVD75 (Kurt J. Lesker Ltd.) coating system at a base pressure around 10^{-6} Torr. A quartz crystal microbalance was used to monitor both the deposition rate, which was fixed at 0.006 nm s^{-1}, and the thickness of the gold film. Once in the spectroelectrochemical cell, first filled with a 10 mM CH_3COONa + 0.1 M $HClO_4$ solution, the gold thin film was gently cycled in the oxygen adsorption/desorption region to eliminate traces of organic molecules and then electrochemically annealed in the same solution by cycling at 20 $mV \cdot s^{-1}$ from 0.05 to 1.20 V for one hour [29]. Then, the cell was flushed with 0.1 M $HClO_4$ solution to

achieve the total removal of acetate anions, which is checked by the absence of the corresponding bands in the ATR-SEIRA spectra. Due to the preferential (111) orientation of the obtained surfaces [29,30], these samples will be noted in the following as Au(111)-25nm.

All the voltammetric and in situ infrared experiments were performed in glass cells using a reversible hydrogen electrode (RHE) as the reference electrode and a gold wire as the counter electrode. The spectroelectrochemical cells used in this work are equipped with a prismatic window (Si or CaF_2, for the internal and external reflection experiments, respectively) beveled at 60° [31,32]. In situ infrared experiments were carried out with a Nexus 8700 (Thermo Scientific) spectrometer equipped with a Veemax (Pike Tech.) reflectance accessory, a MCT-A detector and a wire grid ZnSe polarizer (Pike Tech). All the spectra were collected with a resolution of 8 cm^{-1} and are presented in absorbance units (a.u.) as $-\log(R/R_o)$, where R and R_o represent the single beam sample and reference reflectivity spectra, respectively. Thus, positive-going and negative-going bands correspond, respectively, to gain or loss of species for the sample spectrum with respect to the reference spectrum. Sets of 100 interferograms were collected at different sample potentials and referred to a reference single beam spectrum collected in the HU-containing solutions at 0.10 V. In some ATR-SEIRAS experiments the spectra were collected in a rapid scan mode while the electrode potential was swept at 2 $mV \cdot s^{-1}$. Each spectrum was the average of a set of 104 interferograms which were collected in ten seconds, thus corresponding to a 20 mV interval.

3. Computational details.

Optimized adsorption geometries and harmonic vibrational frequencies of several adsorbates that can plausibly be formed from the reactive adsorption of HU at Au(111) electrodes were obtained from DFT calculations using the Vienna Ab-Initio Simulation Program (VASP, v 4.6) [33-36].

All calculations were carried out with the Projector-Augmented Wave (PAW) method [37] using the pseudopotentials of Kresse and Joubert [38], with a cutoff of 400 eV. The version of Perdew, Burke and Ernzehof [39,40] for the GGA (Generalized Gradient Approximation) functional was used. Spin polarization and van der Waals corrections were not included in the reported calculations.

The slab used to model the Au(111) surface consisted of four layers (9 gold atoms each) with (3x3) surface periodicity. Optimized geometries of the adsorbates were obtained by allowing the relaxation

of the positions of the light atoms. No relaxation of the metal was allowed. The positions of the metal atoms were fixed with the bulk symmetry, and with a metal-metal distance of 0.29520 nm, obtained from the fit to a Murnaghan equation of state using the same PBE functional. The surfaces of neighbouring slab replicas were separated by a vacuum region of more than 12 Angstrom.

Smearing was accomplished with the order-2 Methfessel-Paxton method [41] (with sigma=0.2 eV). For the sampling of the Brillouin zone we used the automatic Monkhorst-Pack [42] method, with a gamma-centered (3 x 3 x 1) scheme. The convergence energy threshold was 10^{-5} eV for the electronic step, and the Hellman-Feynman forces on atoms were required to be below 0.02 eV/Angstrom for the geometry optimization.

For each optimized geometry the harmonic vibrational frequencies were calculated (both for the H- and D-containing adspecies) from the energies corresponding to displacements of +/-0.02 Angstrom in each coordinate. The main contributions to the normal modes corresponding to the calculated vibrational frequencies were visualized using Jmol [43]. The calculated frequencies are reported without any scaling correction. From similar studies in previous work, we can estimate the relative error (in average) of the calculated frequencies to be below 2-3% of the theoretical frequency value.

4. Experimental results.

4.1. Voltammetric experiments.

Panels A and B in Figure 1 show cyclic voltammograms obtained with Au(111) and Au(100) electrodes in contact with perchloric acid solutions with HU concentrations ranging from 0.010 to 10.0 mM. After immersion of the flame-annealed electrode in the working solution at 0.10 V, the electrode potential was cycled from 0.05 to 1.10 V, thus avoiding significant oxidation of the electrode surface. The curves reported in Figure 1A and B correspond to the first voltammetric cycle recorded under these conditions. Figure 1C shows the voltammograms recorded in the first cycle up to 1.10 V with a Au(111)-25nm gold thin film electrode after dosing HU at 0.10 V in the perchloric acid solution. In comparison with the voltammetric response recorded in the HU-free solution, it can be pointed out that no significant extra contribution associated to the presence of HU is detected for potentials below 0.70 V [21] (see also figure S1). Above this potential threshold oxidation currents appear that become higher for increasing HU concentrations. For low HU concentrations, several

current maxima can be observed with peak potentials between 0.70 and 1.10 V. For the higher HU concentrations, a main oxidation peak is observed at ca. 1.0 V, with a shoulder at ca. 0.90 V.

The shape of these voltammetric profiles clearly indicates the chemically irreversible character of the HU electrooxidation. The complexity of the current density pattern suggests the existence of processes involving adsorbed species. The overall shape of the voltammograms is in agreement with the electrooxidation currents being limited by adsorption-related processes. This is especially evident in the case of the Au(100) surface. On this electrode, the positive- and negative-going sweep currents due to HU oxidation are practically coincident (see Figure 1B). As previously reported for (111)-oriented electrodes [21], the observed oxidation currents steadily decrease with continuous cycling between 0.10 and 1.10 V irrespective of the surface orientation (Figure S1). The stationary curves for the Au(111) electrode are reached in the seventh and second cycle when cycling at 50 and 5 $mV \cdot s^{-1}$, respectively (see Figure S2). Besides, the decrease of the voltammetric currents is faster when the lower potential limit is set at higher values, restricting the potential sweep to the range where HU oxidation currents are observed. These behaviors suggest a fast accumulation of adsorbed species which block the surface sites, thus inhibiting the oxidation reaction.

Regarding the structural aspects of HU oxidation at gold electrodes, we can first note that the shape of the voltammetric profile recorded for the gold thin film electrode is similar to that of the Au(111) single crystal electrode, as expected from the preferential (111) orientation of the former. On the other hand, the main difference between the voltammetric behavior of the Au(111) and Au(100) electrodes in the HU-containing solutions is appreciated in the potential region between 0.70 and 0.90 V for HU concentrations up to 1 mM. In this way, a well-marked oxidation peak at 0.82 V is observed for the Au(100) electrode in the 0.1 mM HU solution that is not observed for Au(111). In order to explain the behaviour of the Au(100) sample it must be taken into account that the HU electrooxidation currents may overlap with a voltammetric peak related to the potential-dependent lift of the surface reconstruction characteristic of the flame annealed Au(100) surface [27,28]. This latter process gives rise to the voltammetric feature observed at ca. 0.90 V for the HU-free solution (see curve a in Figure 1B). This feature is known to shift to less positive potentials with increasing concentrations of specifically adsorbed species [27]. This behavior can be also observed in Figure 1B in the HU-containing solutions. For HU concentrations equal or higher than 1 mM, this peak appears as a shoulder of the main HU oxidation currents.

4.2. In situ infrared spectroscopy experiments.

4.2.1. IRRAS experiments with Au(111) and Au(100) electrodes.

Figure 2 shows sets of potential-dependent external-reflection infrared spectra collected with p- or s-polarized light for Au(100) (panels A and B) and Au(111) (panel C) electrodes in a 10 mM HU + 0.1 M $HClO_4$ solution. The spectra were obtained at various electrode potentials from 0.10 V up to 1.10 V (and then down to 0.10 V) by applying ±0.10 V increments and are referred to the single beam spectrum collected, in the same working solution, at 0.10 V just after setting the thin-layer configuration with the flame-annealed electrode. Only some of the spectra collected in the positive-going excursion are shown in the spectral region where well-defined bands appear (i.e. between 2500 and 1900 cm^{-1}). As reported for Au(111) [21], the only features appearing above 2500 cm^{-1} and between 1800 cm^{-1} and the cutoff of the CaF_2 windows are those related to changes in the baseline in the O-H stretching and bending regions of water molecules.

The thin layer configuration used in external reflection experiments helps in the identification of dissolved species which are either trapped or depleted in the space region between the electrode surface and the infrared window (transmission-like experiments). According to the surface selection rule for external reflection experiments [44], the observation of a given absorption band both with s- and p-polarized light indicates that it stems mainly from non-adsorbed species. This is the case for the features at ca. 2345 and 2230 cm^{-1} in the spectra of Figure 2 for both the Au(100) and Au(111) electrodes in the HU-containing solution for potentials above 0.70 V. The band at ca. 2345 cm^{-1} can be assigned to the asymmetric OCO stretching of carbon dioxide and shows for both electrodes a similar potential-dependent behavior (see Figure S3). The band at ca. 2230 cm^{-1} appears also for potentials above 0.70 V (Figure S3) thus being related, as that for CO_2, to the HU electrooxidation reaction. As discussed previously for the Au(111) electrode [21], the band at ca. 2230 cm^{-1} can be assigned either to the N-N stretching of nitrous oxide (N_2O) or to the asymmetric NCO stretching of isocyanic acid. The latter species, which is a weak acid (pKa = 3.77 [45,46]), would be formed in the perchloric acid solution by protonation of adsorbed cyanate anions whose presence is witnessed by an adsorbate band at ca. 2160 cm^{-1} [21].

The feature at ca. 2160 cm^{-1} is only observed in the spectra collected with p-polarised light and appears as a more defined band in the case of the Au(100) (Figure 2A) when compared with Au(111) (Figure 2C) electrode. According to the surface selection rule [44], this latter behavior indicates that this band corresponds to a vibration of an adsorbed species. Moreover, the band frequency is similar

to that of the adsorbate band observed for both Au(111) and Au(100) electrodes in cyanate-containing solutions, which were assigned to the asymmetric NCO stretching of N-bonded cyanate anions on the basis of DFT calculations [47]. According to the plots in Figure S3 for the Au(100) electrode, the intensity of the band at ca. 2160 cm^{-1} first increases and then decreases for potentials above 0.80 V up to 1.10V. In the subsequent negative-going potential excursion (not shown), the band is still observed but with a lower intensity at a given potential than in the positive-going potential excursion. Parallel to the decrease of the integrated intensity of the band at ca. 2160 cm^{-1}, the corresponding band frequency undergoes redshifting (see also Figure S3). This behavior is also typical of adsorbates, that show decreasing band frequencies as a consequence of a lower extent of dipole-dipole coupling when their surface coverage decreases [48-50].

4.2.2. ATR-SEIRAS experiments with gold thin film electrodes.

Figure 3 shows sets of potential-dependent ATR-SEIRA spectra collected for a Au(111)-25nm electrode in a 0.1 M $HClO_4$ solution prepared in water with HU concentrations equal to 0.01, 1.0 and 10 mM. As in the case of the external reflection spectra described above, the electrode potential was changed in a series of steps (by applying ± 0.10 V increments) from 0.10 V (reference potential) up to 1.10 V and then down to 0.10 V. Due to the surface specificity of the SEIRA effect [51], only bands for interfacial species are expected to appear in ATR-SEIRA spectra. Some of the observed bands in Figure 3 are typical of the gold electrode in the perchloric acid solution [52], namely that due to coadsorbed perchlorate anions at 1100 cm^{-1} and those for the bending mode of water around 1650 cm^{-1}, the latter being accompanied by changes in the O-H stretching bands between 3000 and 3700 cm^{-1}. In the spectra for the 0.01 M HU solutions, the potential dependences of these bands are similar to those reported for the pure perchloric acid solution [52]. In this way, the OH bending modes for weakly hydrogen-bonded interfacial water at potentials below the PZC (as for the reference spectrum) appear as a negative-going band at ca. 1610 cm^{-1} whereas strongly hydrogen-bonded water at potentials above the PZC appears as a positive-going band at ca 1650 cm^{-1} [52]. The intensities of the signals of water and perchlorate decrease for HU concentrations higher than 0.01 M, probably due to competition from increasing amounts of adsorbates coming from HU.

A first conclusion from the comparison of the spectra reported in Figure 3 with those obtained in the external reflection experiments described above, is the absence of bands ascribed to solution species (namely, those for carbon dioxide and nitrous oxide (or isocyanic acid)). The latter species, being

formed upon HU oxidation and trapped in the thin solution layer typical of external reflection experiments, can be evacuated easily far from the vicinity of the gold thin film electrode when using the Kretschmann's configuration in the internal reflection experiments. Thus no accumulation of dissolved HU oxidation products is detected in the potential-difference spectra reported in Figure 3. On the contrary, the band at ca. 2160 cm^{-1} assigned above to N-bonded adsorbed cyanate anions is observed for potentials higher than 0.80 V in the 0.01 mM HU solution and for potentials above 0.70 V for higher HU concentrations. The effect of the electrode potential on the band intensity and frequency of this feature is reported in Figure S4 for all the studied HU concentration values. As a difference with results reported in Figure S3, the band intensity steadily increases up to 1.1 V for all the HU concentrations, this behavior being paralleled by a constant blueshift of the band frequency values. Note that the observed band frequency values go well above 2200 cm^{-1} whereas a constant decrease of the latter is observed in the plot shown in Figure S3. As an explanation of this difference, it has to be recalled that the replacement of desorbed cyanate molecules by new adsorbed cyanate molecules formed from dissolved HU molecules is feasible in the Kretschmann's configuration used in the ATR-SEIRAS experiments but not in the thin layer configuration employed in the external reflection experiments. Band intensities and frequencies increase also for a given electrode potential when increasing the HU concentration.

In addition to the adsorbed cyanate band, other positive-going bands can be detected in the spectral region between 1300 and 1900 cm^{-1} in the HU containing solutions with concentrations above 1 mM and for potentials above 0.70 V, that can not be observed in the external reflection spectra. These bands, one around 1810 cm^{-1}, with a shoulder at lower wavenumbers, and a second one at ca. 1405 cm^{-1}, can be related to the existence of various intermediate species formed during the oxidation of HU. Also an absorption band seems to appear at ca 1675 cm^{-1}, thus overlapping with the band for the bending mode of interfacial water at ca. 1650 cm^{-1}.

The interferences from interfacial water bands in the in situ infrared spectra shown in Figure 3 can be avoided by carrying out the ATR-SEIRAS experiments in deuterium oxide solutions. Sets of potential-dependent ATR-SEIRA spectra were obtained in perchloric acid solutions prepared in D_2O with HU concentrations ranging from 0.01 to 10 mM. Some potential-dependent spectra for the 10 mM HU solution are reported in Figure 4. The spectra collected under these conditions show bands for the O-D stretching and bending vibrations that appear, respectively, around 2500 and 1250 cm^{-1}. Even if the former feature overlaps partially with the band of adsorbed cyanate at ca. 2170 cm^{-1}, the spectra obtained in the HU-containing D_2O solutions show effects of the electrode potential and HU concentration on the band intensities and frequencies of this latter feature which are similar to those

reported above in water solutions. On the other hand, Figure 4 shows that the bands in the spectral region between 1300 and 1900 cm^{-1} in the deuterium oxide solution are clearly free from the interferences of OD bending bands. Thus, the bands at 1792 and 1653 cm^{-1} (with shoulders at higher wavenumbers) can be better appreciated. Regarding the band observed at ca. 1403 cm^{-1} in D_2O solution, this feature is also observed at nearly the same wavenumber as in water solutions.

Some of the experiments reported above suggest the existence of processes leading to the accumulation of adsorbates at the gold electrode surface when cycling the electrode potential in the HU-containing solution. In this way, decreasing current densities in successive voltammetric cycles recorded with gold single crystal electrodes are observed in Figure S1. In order to explain this behavior, additional ATR-SEIRAS experiments were carried out in a 10 mM HU+0.1 M $HClO_4$ solution prepared in water. In these experiments the infrared spectra where collected while the electrode potential was slowly cycled several times from 0.10 to 1.10 V and then back to 0.10 V. Figure 5 shows the spectra obtained in the positive- and negative-going sweep during the first, second and fifth cycles. Bands at ca. 2170, 1800 and 1400 cm^{-1} appear and disappear in the spectra as a consequence of the cyclic changes of the electrode potential. Also, a cyclic behavior is observed for the band at ca. 1650 cm^{-1}. Unfortunately, the latter band is overlapped with positive- and negative-going features associated to interfacial water molecules. Besides, since all the spectra are referred to a common single beam spectrum collected at 0.10 V before the first positive-going sweep, a sustained shift of the baseline in the water region gives rise to the development of a positive-going band for water at 1640 cm^{-1}. The plots as a function of the electrode potential of the band intensities for the features at ca. 2170, 1800 and 1400 cm^{-1} are shown in Figure 6. The intensities of all the bands mentioned above increase in the positive-going sweep and, except for the band for adsorbed cyanate (that undergoes a sudden decrease at 1.10 V, probably related to its oxidation to carbon dioxide [47]), still increase while the electrode potential is decreased down to 0.80 V in the subsequent negative-going sweep. At less positive potentials the intensity of all the bands decrease, reaching a zero value at 0.20 V. This latter behavior indicates that adsorbed species being formed in the positive-going sweep are fully desorbed at the end of the negative-going sweep. However, plots in Figure 6 show very important hysteresis, especially those for the bands at 1800 and 1400 cm^{-1}. For these latter features, and for potentials above 0.20-0.30V, the intensity at a given electrode potential is significantly higher in the negative- than in the positive-going sweep. Namely, whereas no significant absorption is detected below 0.70 V in the positive-going sweep, bands are detected in the negative-going sweep down to 0.30 V. The shape of the band intensity vs electrode potential plots also changes with the number of potential cycles, with the bands appearing in the positive-going

sweep at less positive potentials as the number of cycles increases. Note that, in all cycles, the band for adsorbed cyanate (that according to the plots in Figure S3 appears at the same electrode potential as that for carbon dioxide and the one attributable to isocyanic acid and/or nitrous oxide) is observed at slightly lower potentials than those for the bands between ca. 1300 and 1900 cm^{-1} (0.70 V vs ca. 0.80-0.90 V). However, the onset for the development of these latter features is observed at potentials below that for the maximum cyanate band intensity (around 1.10 V). It has to be also noted that all the changes in the band intensity plots shown in Figure 6 are essentially paralleled by changes in the corresponding plots for the band frequency (see Figure S5). Higher band intensities imply higher band frequencies. In the case of the feature at 1780-1810 cm^{-1}, the plots in Figure S5 (which show the potential-dependent behavior of the band frequency of the more intense feature in this spectral region) clearly show the existence of two contributions and the changes of their relative intensities as a function of the electrode potential. The contribution above 1800 cm^{-1} predominates at potentials above 0.70 V, whereas that around 1785 cm^{-1} predominates for potentials between 0.70 and 0.30 V in the negative-going sweep. An apparent discontinuity is observed in the frequency-potential plot for the band at ca. 1800 cm^{-1}. This only reflects that below that particular potential value the highest absorption corresponds to the the lowest wavenumber of the two partially overlapped signals.

5. DFT results.

DFT calculations were carried out in order to obtain optimized adsorption geometries (see Figure 7 and Table 1) and theoretical harmonic vibrational frequencies (shown in Table 2) for six different species that can be formed from HU while keeping the NCN skeleton. These include the molecule of HU itself (adspecies I), as well as five other adsorbed species that can be generated from HU in a sequence of oxidation steps (each one involving the loss of one proton and one electron). Formation of adspecies II to IV would involve the breaking of N-H bonds as previously reported for the adsorption of urea on platinum [11,15] and gold [12] electrodes. In the case of HU we have also considered the oxidative loss of the H atom in the OH moiety, to form a nitroso compound (adsorbed nitrosoformamide (adspecies V) or its deprotonated form (adspecies VI)), as this functional group has been reported to be formed as a consequence of HU oxidation [5-9]. Scheme I shows the reaction network that links through monoelectronic redox reactions the six adsorbed species considered in our calculations.

Table 1 summarizes the N-Au distances (both for $–NH_x$ and –NO) measured for these optimized geometries. The values can be divided in three ranges, depending on whether the N-Au bond can be considered as covalent, dative (involving lone pairs of the nitrogen atom) or nonexistent. The shortest distances correspond to the first case, with values between 215 and 224 pm. Slightly longer distances (ranging from 238 to 299 pm) correspond to the weaker, dative bond. Finally, in the absence of N-Au bonding, the N-Au distances are around 350 pm, too long for a chemical bond interaction.

Regarding the tilting of the Au-N bonds with respect to the normal to the metal surface, the angles in all cases are below 10º, except for HU, with a value close to 12º. A more significant geometric parameter is the tilting of the molecular plane (that of the NCN skeleton) of the adsorbate with respect to the normal. In all cases, except for HU, this tilting is below 45º. This means that vibrations of these adsorbates can have a non-negligible component of the transition dipole in the direction perpendicular to the metal surface, thus making feasible their identification by in-situ surface IR techniques both under external reflection conditions [44] and in ATR-SEIRAS experiments [53]. For HU the tilting is much greater, with the molecular plane being not far from parallel to the surface. This adds to its weak interaction with the metal, reinforcing the conclusion about its irrelevance for the assignment of the recorded experimental bands.

The calculated harmonic frequency values between 1900 and 1300 cm^{-1} for both H- and D-containing (values in brackets) species are summarized in Table 2, where they can be compared with experimental values from the ATR-SEIRA spectra collected at 1.0 V in the 10 mM HU solution. Note that the replacement of hydrogen by deuterium in D_2O solutions is expected due to the acid-base equilibria involving the N-H and O-H groups in hydroxyurea.

6. Discussion.

The spectroelectrochemical results reported in this work have shown that HU electrooxidation proceeds at gold electrodes above 0.70 V RHE, as a fully irreversible, complex oxidation process. Voltammetric current profiles indicate that the oxidation currents are limited by adsorption processes, not being limited by mass transport (diffusion) in the solution. This is especially evident for the Au(100) electrode with a nearly identical current response in the negative- and positive-going sweep directions (between 0.10 and 1.10 V RHE). Experimental evidences strongly indicate the formation of adsorbed species that can contribute to the observed decrease of the HU

electrooxidation currents with potential cycling and that rapidly accumulate on the electrode surface when the negative-going voltammetric sweep is restricted to potentials higher than 0.70 V.

Two main aspects of the experimental espectroelectrochemical results reported in this work have to be considered for discussion. The first one is related to the main reaction products formed during HU electrooxidation at gold electrodes that can be identified in the IRRAS experiments. The second point to consider is the nature of intermediate species detected from the ATR-SEIRA data in the light of the DFT calculations for HU and related species.

The external reflection IR experiments with Au(100) and Au(111) electrodes have clearly shown the formation, as products of the irreversible oxidation of HU, of dissolved CO_2 (trapped in the solution thin-layer) as well as adsorbed (N-bonded) cyanate (confirmed by the intense bands appearing in the ATR-SEIRA spectra). An absorption band at ca. 2230 cm^{-1} can be assigned either to dissolved isocyanic acid (HNCO) (formed from the protonation of adsorbed cyanate) or to N_2O (formed from the oxidation of hydroxylamine, the latter species being formed together with cyanate anions upon HU dissociation). These observations suggest the existence of a complex mechanism with several parallel paths involving the dissociation of HU to adsorbed cyanate (that can protonate to yield dissolved isocyanic acid) and hydroxylamine (readily oxidized at gold electrodes to nitrous oxide [24])

$$H_2NCONHOH \rightarrow OCN^-(ads) + NH_2OH + H^+ \quad (1)$$

$$2\ NH_2OH \rightarrow N_2O + H_2O + 4H^+ + 4e \quad (2)$$

We can consider also the direct oxidation of HU to carbon dioxide and hydroxylamine (followed by reaction (2))

$$H_2NCONHOH + 2\ H_2O \rightarrow CO_2 + 2\ NH_2OH + 2\ H^+ + 2\ e \quad (3)$$

Whereas carbon dioxide and nitrous oxide have been detected as products of the chemical oxidation of HU [5-9], the formation of cyanate can be favoured during the electrooxidation of HU due to its strong adsorption at gold electrodes. The formation of nitrosoformamide,

$$H_2NCONHOH \rightarrow H_2NCONO + 2\ H^+ + 2\ e \quad (4)$$

found as intermediate under chemical oxidation conditions [5-9], and proposed as the dissolved oxidation product of HU at carbon paste electrodes [18,19], can not be confirmed from our IRRAS experiments. It has to be remarked that nitrosoformamide in solution has been proposed to hydrolyze to HNO and carbamic acid (NH_2COOH), which would readily decompose to carbon dioxide and ammonia [6,8].

The strong exaltation due to the SEIRA effect has allowed the recording of several well-defined IR peaks in the region between 1300 and 1900 cm^{-1} for the Au(111)-25nm thin layer electrodes which provide strong experimental evidences for the formation of adsorbed species other than N-bonded cyanate. From the data in Table 2 it can be concluded that none of the recorded IR signals (appearing around 1800, 1650 and 1400 cm^{-1} in the experiments carried out in water, with very slight shifts when using deuterium oxide as the solvent) can be assigned to the vibrational modes of adsorbed hydroxyurea (adspecies I). Calculated wavenumbers (for the non-deuterated species) appear at 1712, 1572, 1498 and 1375 cm^{-1}. This, together with the weak HU-metal interaction and very strong tilting of the molecular plane seems to exclude adsorbed HU from being at the origin of any of the experimental IR bands.

After discarding adspecies I, we will focus on the eventual assignment of the experimental adsorbate bands (other than cyanate) to species II to VI. The feature appearing around 1800 cm^{-1} can be clearly assigned to the stretching of the carbonyl group of adspecies V and VI (i.e. those with a nitroso group, NH_xCONO (with x=2 or 1), with calculated values of 1810 and 1792 cm^{-1} and almost negligible shifts upon deuteration. These species correspond in fact to nitrosoformamide, detected here in the adsorbed (eventually deprotonated) form

$$H_2NCONHOH \rightarrow H_2NCONO(ads) + 2\,H^+ + 2\,e \qquad (5)$$

$$H_2NCONO(ads) \rightarrow HNCONO(ads) + H^+ + e \qquad (6)$$

From the spectroscopic results reported in this work it can be stated that adsorbed nitrosoformamide species persist at the gold electrode surface at least for potentials below 1.10 V.

Several species have theoretical frequencies relatively close to 1650 cm^{-1}. First of all, the NO stretching band for species V (1591 cm^{-1}) and VI (1620 cm^{-1}) lie in this spectral region, although the corresponding dynamic dipoles are almost parallel to the electrode surface (specially for species V).

Other candidates for explaining the bands at ca. 1650 cm^{-1} are the CO stretching modes of adspecies II (1684 cm^{-1}), III (1620 cm^{-1}), and IV (1650 cm^{-1}). All these values agree reasonably with the experimental ones, as the discrepancy amounts to around 2% of the experimental value, which in turn has an uncertainty estimated in 8 cm^{-1}. Note also that the calculated CO stretching frequencies are similar to those obtained for adsorbed ureylene (deprotonated N-bonded urea, NHCONH) species at Pt(100) surfaces by García-Hernández et al. [54], that validated previous assignments of the infrared bands observed experimentally for Pt(100) electrodes in acidic urea-containing solutions [11]. These assignments were based on a comparison with the spectra reported for urea coordination compounds, for which the corresponding CO and NCN stretching frequencies were related to bonding either through the N atom (CO stretching bands above ca. 1600 cm^{-1}) or through the O atom (CO stretching bands below ca. 1600 cm^{-1}) [55-57].

Discriminating species II to VI from vibrational bands other than the CO stretching band is complicated in some cases by the orientation of the corresponding dynamic dipole, which is almost parallel to the electrode surface. This is the case of the NH_2 bending mode for species III and V and the N-OH bending for adspecies II, III and IV (see Figure 7). The same holds for the asymmetric NCN stretching for species II to IV and VI. Besides, the calculated frequency values lie in a region in the experimental spectra which is obscured by the interferences from spurious absorption due to uncompensated Si-O bands coming from the silicon prism and from co-adsorbed perchlorate bands.

The most problematic assignment is that for the bands appearing around 1400 cm^{-1} in the spectra collected both in water and deuterium oxide. The adspecies (apart from I) having theoretical frequencies relatively close to that value are species II (1464 cm^{-1}) and III (1412 cm^{-1}), being both related to the NOH bending mode. However, in both cases these values are strongly shifted upon deuteration (to 1260 and 1151 cm^{-1} respectively). In any case, the possible presence of adspecies II and III can not be ruled out, as it could be argued that the signals for the deuterated species could overlap with the experimental Si-O and co-adsorbed perchlorate signals (see above). In any case, the features around 1400 cm^{-1} in D_2O cannot be explained on the basis of the calculated values reported here.

A possibility for the interpretation of these features could be their assignment to species being formed from adsorbed cyanate, which is formed from the dissociative adsorption of hydroxyurea (reaction (1)). As previously discussed, in the presence of high concentrations of cyanate anions, the formation of adsorbed monocyanurate anions (coming from the dissociation of cyanuric acid, which can be considered as a trimer of isocyanic acid) has been proved at gold electrode surfaces [58,59].

Characteristic bands in the ATR-SEIRA spectra obtained both in cyanate and in cyanuric acid solutions include well-marked features at ca. 1450 and 1400 cm^{-1} assigned, respectively, to the asymmetric and symmetric NCN stretch of the adsorbed monocyanurate anions. In addition, CO stretching bands for adsorbed monocyanurate appear in the range between 1743-1780 cm^{-1} in a 10 mM cyanate solution, being observed at 1770-1793 cm^{-1} for a higher monocyanurate coverage reached in a 10 mM cyanuric acid solution (working solutions being both prepared in 0.08 M $NaClO_4$ as supporting electrolyte) [58,59]. Differences between the spectra obtained in cyanate/cyanurate and HU-containing solutions (a single band around 1400 cm^{-1} and higher CO stretching frequencies in the spectra collected for the gold thin film electrode in HU-containing solutions) can not be ascribed to the differences in the solution pH since similar spectra to those reported in this work are obtained for gold electrodes in contact with HU-containing sodium perchlorate solutions. On the other hand, and despite of the high cyanate coverage reached during HU oxidation, the differences mentioned above between the spectra collected in cyanuric acid- and HU-containing solutions (that includes the absence in the latter case of a band observed at ca. 1580 cm^{-1} for the asymmetric OCNCO stretching of adsorbed monocyanurate [59]) seems to support that bands observed in the HU-containing solutions are not related to the formation of monocyanurate anions from adsorbed cyanate.

Another point open to discussion is the analysis of the fine structure of the features near 1800, 1650 and 1400 cm^{-1} in the spectra obtained in the HU-containing solutions. We have not attempted such a detailed analysis of the broadening and splitting of experimental bands, because the presence of different peaks (or shoulders) in a given spectral region can be due not only to the existence of different species but also to other phenomena. These include the formation of hydrogen bonds [60-62] that can occur intramolecularly, between neighbouring adsorbates (that can differ in chemical composition), or between adsorbates and interfacial water, as well as the extent of dipole-dipole coupling in collective modes at high adsorbate coverages [48-50] in wide adlayer domains. Moreover, the complexity of the adsorbate layer, with different adsorbates coexisting at each potential with different adsorbate coverages, leads to a very rich variety of microscopical configurations. Some of these configurations could perhaps explain the observation of the signal at 1400 cm^{-1} in deuterated water – though the possibility of other chemical species not considered here cannot be discarded a priori. A complete systematic study of these effects with the different adsorbates considered would require a great volume of computations, and is out of the scope of this work. On this basis, from the frequency values reported, our band assignments should be considered as tentative.

7. Conclusions.

Spectroelectrochemical experiments reported in this work have shown than HU oxidizes irreversibly at gold electrodes, the electrode reaction being limited by adsorption processes that contribute to the steady decrease of the electrooxidation current during the voltammetric experiments. In situ IRRAS experiments suggest the existence of parallel oxidation paths leading to the formation of adsorbed cyanate and hydroxylamine or carbon dioxide and hydroxylamine. This latter molecule is highly unstable at gold electrodes in the potential range for HU oxidation, giving rise to the formation of nitrous oxide, which could be at the origin of the spectral feature appearing at ca. 2230 cm^{-1}. This band could also be related to the presence of dissolved isocyanic acid, formed by protonation of adsorbed cyanate anions.

The ATR-SEIRA spectra reported in this work confirm the formation of adsorbed cyanate anions during HU oxidation, showing a variety of bands in the spectral region between 1300 and 1900 cm^{-1} that could be related to intermediate species of the HU electrooxidation reaction. The weak bonding of HU to the Au(111) model surface, evidenced by the long N-Au distance, together with the strong tilting of the NCN plane and the strong discrepancy between the calculated frequencies for its vibrational modes and those of the experimental bands allow to conclude that it its highly unlikely that HU contributes to the recorded surface spectra. Instead, we have interpreted these IR signals, on the basis of the calculated geometries and harmonic theoretical frequencies for several adsorbates derived from HU by loss of one or more H atoms (coupled to electron transfer) without breaking the NCN backbone. The experimental bands around 1800 cm^{-1} found both in water and in deuterium oxide correspond to the CO stretching of adsorbates having a nitrosyl group formed by oxidation of the NOH moiety that can be identified from DFT results either as adsorbed nitrosoformamide or its deprotonated form. The signals around 1650 cm^{-1} do not have straightforward an unequivocal assignment as they can be due either to the NO stretch of the former species or to the CO stretch of different species conserving the NOH group. The full discrimination of contributions from these adspecies in the infrared spectra and their potential-dependent interconversion is not possible from the present data due to the similarity of the calculated band frequencies for their various vibrational modes.

The most problematic assignment is that of the experimental signal at 1400 cm^{-1}. This signal, as those around 1650 and 1800 cm^{-1}, shifts marginally upon deuteration. However, the calculated frequencies obtained for adsorbed species around 1400 cm^{-1} are expected to significantly redshift

upon deuteration. The high complexity of the actual experimental system, with several adsorbates that may interact (among them and with interfacial water molecules) through hydrogen bonding makes unfeasible a fully realistic modelisation that could explain conclusively the assignment of that IR signal.

Acknowledgements.

Prof. Juan M. Feliu is acknowledged for providing the gold single crystal electrodes used in this work. The authors acknowledge the funding by Ministerio de Economía y Competitividad through projects CTQ2016-76221-P (AIE/FEDER, UE) and CTQ2016-76231-C2-2-R (AEI/FEDER, UE) and by the University of Alicante (VIGROB-263). William Cheuquepán is grateful for the award of a F.P.I. grant associated to project CTQ2009-13142.

Reference List

1. G. Yasaki, Y. Xu, and S. B. King, "*An efficient synthesis of 15N-hydroxyurea*", Synth. Commun., 30 (2000) 2041-2047.
2. S. B. King, "*The nitric oxide producing reactions of hydroxyurea*", Curr. Med. Chem., 10 (2003) 437-452.
3. P. Kovacic, "*Hydroxyurea (therapeutics and mechanism): Metabolism, carbamoyl nitroso, nitroxyl, radicals, cell signaling and clinical applications*", Med. Hypotheses, 76 (2011) 24-31.
4. D. G. H. Silva, E. Belini, Jr., G. C. de Souza Carrocini, L. de Souza Torres, O. Ricci, Jr., C. L. de Castro Lobo, C. R. Bonini-Domingos, and E. A. de Almeida, "*Genetic and biochemical markers of hydroxyurea therapeutic response in sickle cell anemia*", BMC Med. Genet., 14 (2013) 108.
5. J. Huang, E. M. Sommers, D. B. Kim-Shapiro, and S. B. King, "*Horseradish peroxidase catalyzed nitric oxide formation from hydroxyurea*", J. Am. Chem. Soc., 124 (2002) 3473-3480.
6. N. Kujundzic, B. Nigovic, and K. Sankovic, "*Reaction of hydroxyurea with iron(III): Products and the stoichiometry of the redox reaction*", Z. Anorg. Allg. Chem., 630 (2004) 2749-2753.
7. M. Gabricevic, E. Besic, M. Birus, A. Zahl, and R. van Eldik, "*Oxidation of hydroxyurea with oxovanadium(V) ions in acidic aqueous solution*", J. Inorg. Biochem., 100 (2006) 1606-1613.
8. A. Budimir, E. Besic, and M. Birus, "*Kinetics and mechanism of oxidation of hydroxyurea with hexacyanoferrate(III) ions in aqueous solution*", Croat. Chem. Acta, 82 (2009) 807-818.
9. D. Chatterjee, K. A. Nayak, E. Ember, and R. van Eldik, "*[RuIII(edta)(H2O)]-mediated oxidation of hydroxyurea with H_2O_2. Kinetic and mechanistic investigation*", Dalton Trans., 39 (2010) 1695-1698.
10. M. Rubel, C. K. Rhee, A. Wieckowski, and P. A. Rikvold, "*Cyclic voltammetry of platinum single crystal electrodes in solutions containing urea*", J. Electroanal. Chem., 315 (1991) 301-306.
11. V. Climent, A. Rodes, J. M. Orts, J. M. Feliu, J. M. Pérez, and A. Aldaz, "*On the electrochemical and in-situ Fourier transform infrared spectroscopy characterization of urea adlayers at Pt(100) electrodes*", Langmuir, 13 (1997) 2380-2389.
12. M. Nakamura, M. B. Song, and M. Ito, "*Adsorption of urea on Au(100) and Au(111) electrode surfaces studied by in-situ Fourier-transform infra-red spectroscopy*", Surf. Sci., 428 (1999) 167-172.
13. V. Climent, A. Rodes, J. M. Pérez, J. M. Feliu, and A. Aldaz, "*Urea adsorption at rhodium single-crystal electrodes*", Langmuir, 16 (2000) 10376-10384.
14. V. Climent, A. Rodes, R. Albalat, J. Claret, J. M. Feliu, and A. Aldaz, "*Urea adsorption on platinum single crystal stepped surfaces*", Langmuir, 17 (2001) 8260-8269.
15. V. Climent, A. Rodes, J. M. Orts, A. Aldaz, and J. M. Feliu, "*Urea adsorption on Pt(111) electrodes*", J. Electroanal. Chem., 461 (1999) 65-75.
16. V. Climent, A. Rodes, J. M. Orts, J. M. Feliu, and A. Aldaz, "*The electrochemistry of nitrogen-containing compounds at platinum single crystal electrodes: Part 2. Semicarbazide on Pt(100) electrodes*", J. Electroanal. Chem., 436 (1997) 245-255.

17. V. Climent, A. Rodes, J. M. Orts, J. M. Feliu, and A. Aldaz, "*The electrochemistry of nitrogen-containing compounds at platinum single crystal electrodes - Part 3. Carbohydrazide on Pt(hkl) electrodes*", J. Electroanal. Chem., 467 (1999) 20-29.
18. K. M. Naik, M. M. Alagur, and S. T. Nandibewoor, "*Electrochemical response of hydroxyurea by different voltammetric techniques at carbon paste electrode*", Anal. Methods, 5 (2013) 6947-6953.
19. K. M. Naik, C. R. Ashi, and S. T. Nandibewoor, "*Anodic voltammetric behavior of hydroxyurea and its electroanalytical determination in pharmaceutical dosage form and urine*", J. Electroanal. Chem., 755 (2015) 109-114.
20. B. Nigovic, N. Kujundzic, and K. Sankovic, "*Electron transfer in N-hydroxyurea complexes with iron(III)*", Eur. J. Med. Chem., 40 (2005) 51-55.
21. W. Cheuquepán, J. M. Orts, A. Rodes, and J. M. Feliu, "*Voltammetric and in situ infrared spectroscopy studies of hydroxyurea electrooxidation at Au(111) electrodes in $HClO_4$ solutions*", Electrochem. Commun., 76 (2017) 34-37.
22. F. Kitamura, M. Takahashi, and M. Ito, "*Anodic oxidation of cyanide and cyanate ions on a platinum electrode*", Chem. Phys. Lett., 136 (1987) 62-66.
23. O. Yépez and B. R. Scharifker, "*Mechanistic pathways during oxidation of cyanate on platinum single crystal faces*", Electrochim. Acta, 50 (2005) 1423-1429.
24. A. J. J. Jebaraj, D. Kumsa, and D. A. Scherson, "*Oxidation of hydroxylamine on gold electrodes in aqueous electrolytes: rotating ring-disk and in situ Infrared Reflection Absorption Spectroscopy studies*", J. Phys. Chem. C, 116 (2012) 6932-6942.
25. J. Clavilier, D. Armand, S.-G. Sun, and M. Petit, "*Electrochemical adsorption behaviour of platinum stepped surfaces in sulphuric acid solutions*", J. Electroanal. Chem., 205 (1986) 267-277.
26. A. Rodes, E. Herrero, J. M. Feliu, and A. Aldaz, "*Structure sensitivity of irreversibly adsorbed tin on gold single-crystal electrodes in acid media*", J. Chem. Soc. Faraday. Trans., 92 (1996) 3769-3776.
27. D. M. Kolb, "*Reconstruction phenomena at metal-electrolyte interfaces*", Prog. Surf. Sci., 51 (1996) 109-173.
28. A. Hamelin, "*Cyclic voltammetry at gold single-crystal surfaces .1. Behaviour at low index faces*", J. Electroanal. Chem., 407 (1996) 1-11.
29. J. M. Delgado, J. M. Orts, J. M. Pérez, and A. Rodes, "*Sputtered thin-film gold electrodes for in situ ATR-SEIRAS and SERS studies*", J. Electroanal. Chem., 617 (2008) 130-140.
30. T. Wandlowski, K. Ataka, S. Pronkin, and D. Diesing, "*Surface enhanced infrared spectroscopy-Au(111-20 nm)/sulphuric acid - new aspects and challenges*", Electrochim. Acta, 49 (2004) 1233-1247.
31. A. Rodes, J. M. Pérez, and A. Aldaz, *"Vibrational Spectroscopy"*, in Handbook of Fuel Cells. Fundamentals, Technology and Applications., Vielstich, W., Gasteiger, H. A., and Lamm, A. (Eds.), John Wiley & Sons Ltd., Chichester, 2003, 191-219.
32. J. M. Delgado, J. M. Orts, and A. Rodes, "*ATR-SEIRAS study of the adsorption of acetate anions at chemically deposited silver thin film electrodes*", Langmuir, 21 (2005) 8809-8816.
33. G. Kresse and J. Hafner, "*Ab initio molecular dynamics of liquid metals*", Phys. Rev. B: Condens. Matter, 47 (1993) 558-561.
34. G. Kresse and J. Hafner, "*Ab initio molecular-dynamics simulation of the liquid-metal-amorphous-semiconductor transition in germanium*", Phys. Rev. B: Condens. Matter, 49 (1994) 14251-14269.

35. G. Kresse and J. Furthmueller, "*Efficient iterative schemes for ab initio total-energy calculations using a plane-wave basis set*", Phys. Rev. B: Condens. Matter, 54 (1996) 11169-11186.
36. G. Kresse and J. Furthmuller, "*Efficiency of ab-initio total energy calculations for metals and semiconductors using a plane-wave basis set*", Comput. Mater. Sci., 6 (1996) 15-50.
37. P. E. Bloechl, "*Projector augmented-wave method*", Phys. Rev. B: Condens. Matter, 50 (1994) 17953-17979.
38. G. Kresse and D. Joubert, "*From ultrasoft pseudopotentials to the projector augmented-wave method*", Phys. Rev. B: Condens. Matter Mater. Phys., 59 (1999) 1758-1775.
39. J. P. Perdew, K. Burke, and M. Ernzerhof, "*Generalized gradient approximation made simple*", Phys. Rev. Lett., 77 (1996) 3865-3868.
40. J. P. Perdew, K. Burke, and M. Ernzerhof, "*Generalized gradient approximation made simple. [Erratum to document cited in CA126:51093]*", Phys. Rev. Lett., 78 (1997) 1396.
41. M. Methfessel and A. T. Paxton, "*High-precision sampling for Brillouin-zone integration in metals*", Phys. Rev. B: Condens. Matter, 40 (1989) 3616-3621.
42. H. J. Monkhorst and J. D. Pack, "*Special points for Brillouin-zone integrations*", Physical Review B-Condensed Matter, 13 (1976) 5188-5192.
43. "*Jmol: an open-source Java viewer for chemical structures in 3D.*", http://www. jmol. org, (2015).
44. R. G. Greenler, "*Infrared study of adsorbed molecules on metal surfaces by reflection techniques*", J. Chem. Phys., 44 (1966) 310-315.
45. D. J. Belson and A. N. Strachan, "*Preparation and properties of isocyanic acid*", Chem. Soc. Rev., 11 (1982) 41-56.
46. K. Adamczyk, J. Dreyer, D. Pines, E. Pines, and E. T. J. Nibbering, "*Ultrafast protonation of cyanate anion in aqueous solution*", Isr. J. Chem., 49 (2009) 217-225.
47. W. Cheuquepán, J. M. Orts, A. Rodes, and J. M. Feliu, "*DFT and spectroelectrochemical study of cyanate adsorption on gold single crystal electrodes in neutral medium*", J. Electroanal. Chem., (2016) http://dx.doi.org/10.1016/j.jelechem.2016.10.011.
48. M. W. Severson, C. Stuhlmann, I. Villegas, and M. J. Weaver, "*Dipole-dipole coupling effects upon infrared spectroscopy of compressed electrochemical adlayers: application to the Pt(111)/CO system*", J. Chem. Phys., 103 (1995) 9832-9843.
49. D. Loffreda, D. Simon, and P. Sautet, "*Dependence of stretching frequency on surface coverage and adsorbate-adsorbate interactions: a density-functional theory approach of CO on Pd (111)*", Surf. Sci., 425 (1999) 68-80.
50. D. Curulla, A. Clotet, and J. M. Ricart, "*Adsorption of carbon monoxide on Pt{100} surfaces: dependence of the CO stretching vibrational frequency on surface coverage*", Surf. Sci., 460 (2000) 101-111.
51. M. Osawa, "*Dynamic processes in electrochemical reactions studied by Surface-Enhanced Infrared Absorption Spectroscopy (SEIRAS)*", Bull. Chem. Soc. Jpn., 70 (1997) 2861-2880.
52. K. Ataka, T. Yotsuyanagi, and M. Osawa, "*Potential-dependent reorientation of water molecules at an electrode/e lectrolyte interface studied by surface-enhanced infrared absorption spectroscopy*", J. Phys. Chem., 100 (1996) 10664-10672.
53. M. Osawa, K. Ataka, K. Yoshii, and Y. Nishikawa, "*Surface-Enhanced Infrared Spectroscopy : the origin of the absorption enhancement and band selection rule in the*

infrared spectra of molecules adsorbed on fine metal particles", Appl. Spectrosc., 47 (1993) 1497-1502.
54. H. M. García, U. Birkenheuer, A. G. Hu, F. Illas, and N. Rosch, "*Theoretical study of the adsorption of urea related species on Pt(100) electrodes*", Surf. Sci., 471 (2001) 151-162.
55. R. B. Penland, S. Mizushima, C. Curran, and J. V. Quagliano, "*Infrared absorption spectra of inorganic coordination complexes. X. Studies of some metal-urea complexes*", J. Am. Chem. Soc., 79 (1957) 1575-1578.
56. T. Theophanides and P. D. Harvey, "*Structural and spectroscopic properties of metal-urea complexes*", Coord. Chem. Rev., 76 (1987) 237-264.
57. T. C. Woon, W. A. Wickramasinghe, and D. P. Fairlie, "*Oxygen versus nitrogen coordination of a urea to (diethylenetriamine)platinum(II)*", Inorg. Chem., 32 (1993) 2190-2194.
58. W. Cheuquepán, A. Rodes, J. M. Orts, and J. M. Feliu, "*Formation of cyanuric acid from cyanate adsorbed at gold electrodes*", Electrochem. Commun., 74 (2017) 1-4.
59. W. Cheuquepán, A. Rodes, J. M. Orts, and J. M. Feliu, "*Spectroelectrochemical detection of specifically adsorbed cyanurate anions at gold electrodes with (111) orientation in contact with cyanate and cyanuric acid neutral solutions*", J. Electroanal. Chem., (2017) http://dx.doi.org/10.1016/j.jelechem.2017.02.015.
60. A. P. Sandoval, J. M. Orts, A. Rodes, and J. M. Feliu, "*Adsorption of glycine on Au(hkl) and gold thin film electrodes: an in situ spectroelectrochemical study*", J. Phys. Chem. C, 115 (2011) 16439-16450.
61. A. P. Sandoval, J. M. Orts, A. Rodes, and J. M. Feliu, "*A comparative study of the adsorption and oxidation of L-alanine and L-serine on Au(100), Au(111) and gold thin film electrodes in acid media*", Electrochim. Acta, 89 (2013) 72-83.
62. W. Cheuquepán, J. M. Pérez, J. M. Orts, and A. Rodes, "*Spectroelectrochemical and DFT Study of Thiourea Adsorption on Gold Electrodes in Acid Media*", J. Phys. Chem. C, 118 (2014) 19070-19084.

Figure captions.

Figure 1. Cyclic voltammograms obtained for A) Au(111), B) Au(100) and C) Au(111)-25nm electrodes during the first voltammetric cycle between 0.05 and 1.10 V in a x mM HU + 0.1 M $HClO_4$ solutions. x= a) 0, b) 0.01; c) 0.1 d) 1 and e) 10. Sweep rate: 50 $mV \cdot s^{-1}$.

Figure 2. Potential-dependent infrared external reflection spectra collected with p- (A,C) or s- (B) polarized light for A,B) Au(100) and C) Au(111) electrodes in a 10 mM HU+0.1 M $HClO_4$ solution. The reference spectrum was collected at 0.10 V in the same solution. 100 interferograms were coadded to obtain each single beam spectrum.

Figure 3. Potential-dependent ATR-SEIRA spectra collected with p-polarized light for a Au(111)-25nm electrode in a x mM HU+0.1 M $HClO_4$ solution prepared in water. A) x= 0.01; B) x= 1 C) x=10. The reference spectrum was collected at 0.10 V in the same solution. 100 interferograms were coadded to obtain each single beam spectrum. The inset in panel C shows an expanded view of the spectra collected at some electrode potentials in the 10 mM HU-containing solution.

Figure 4. Potential-dependent ATR-SEIRA spectra collected with p-polarized light for a Au(111)-25nm electrode in a 10 mM HU+0.1 M $HClO_4$ solution prepared in deuterium oxide. The reference spectrum was collected at 0.10 V in the same solution. 100 interferograms were coadded to obtain each single beam spectrum.

Figure 5. Potential-dependent ATR-SEIRA spectra collected with p-polarized light during the first, second and fifth cycle between 0.10 and 1.10 V at 2.0 mV/s. Each spectrum was referred to a single beam spectrum collected at 0.10 V before the potential cycles and is the average of 103 interferograms.

Figure 6. Plots for the potential-dependent integrated band intensities of adsorbate bands at ca. 2180, 1800 and 1400 cm^{-1} in the ATR-SEIRA spectra collected with a Au(111)-25 nm electrode in 1mM HU + 0.1 M $HClO_4$ solutions between 0.1 and 1.10 V (first (■), second (○) and fifth (★) positive- and negative-going sweeps).

Figure 7. Optimized adsorption geometries at Au(111) of HU and some intermediates formed by partial electrooxidation of HU.

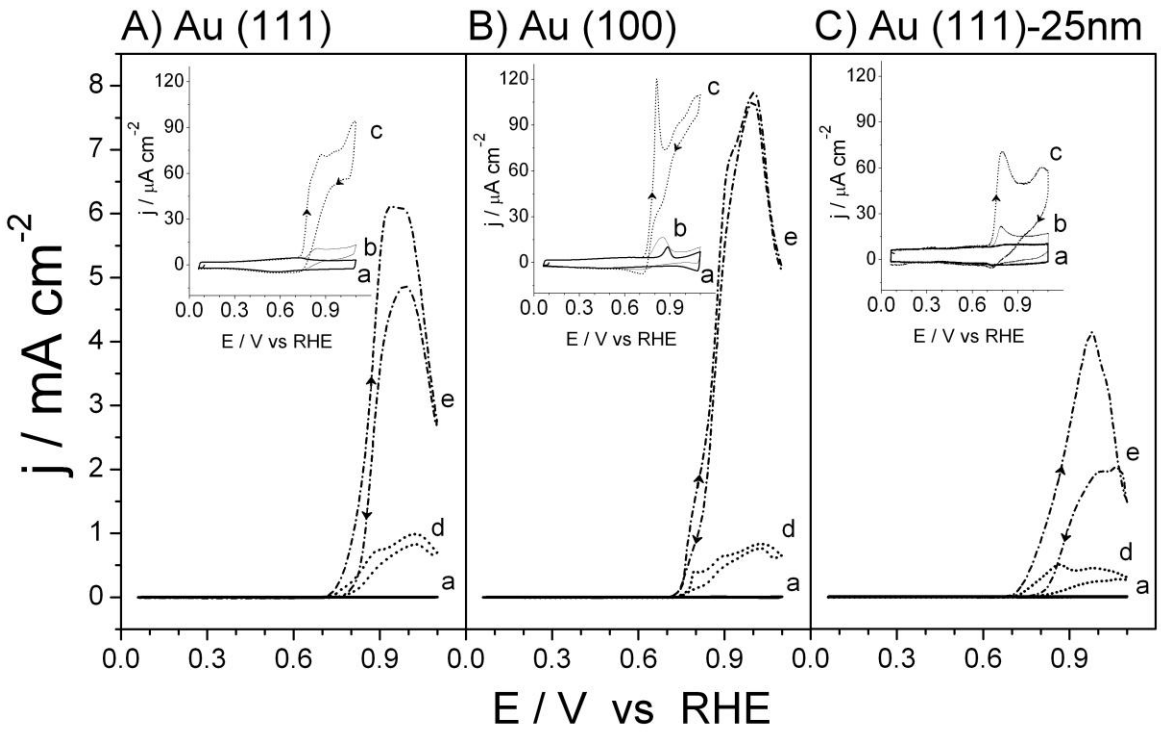

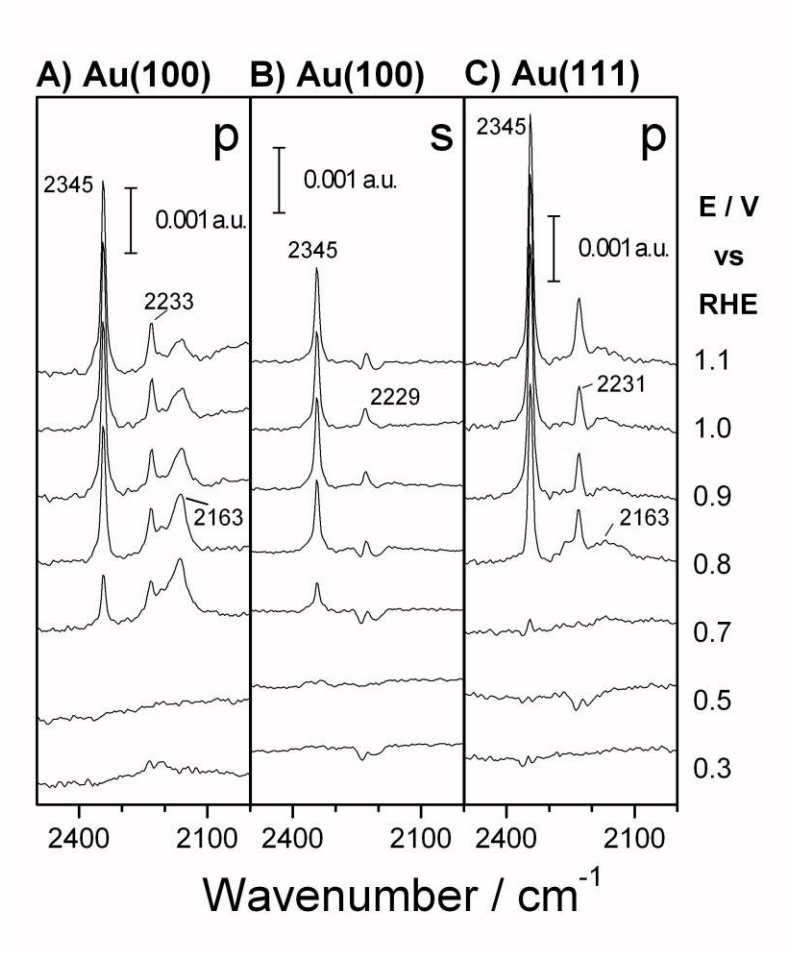

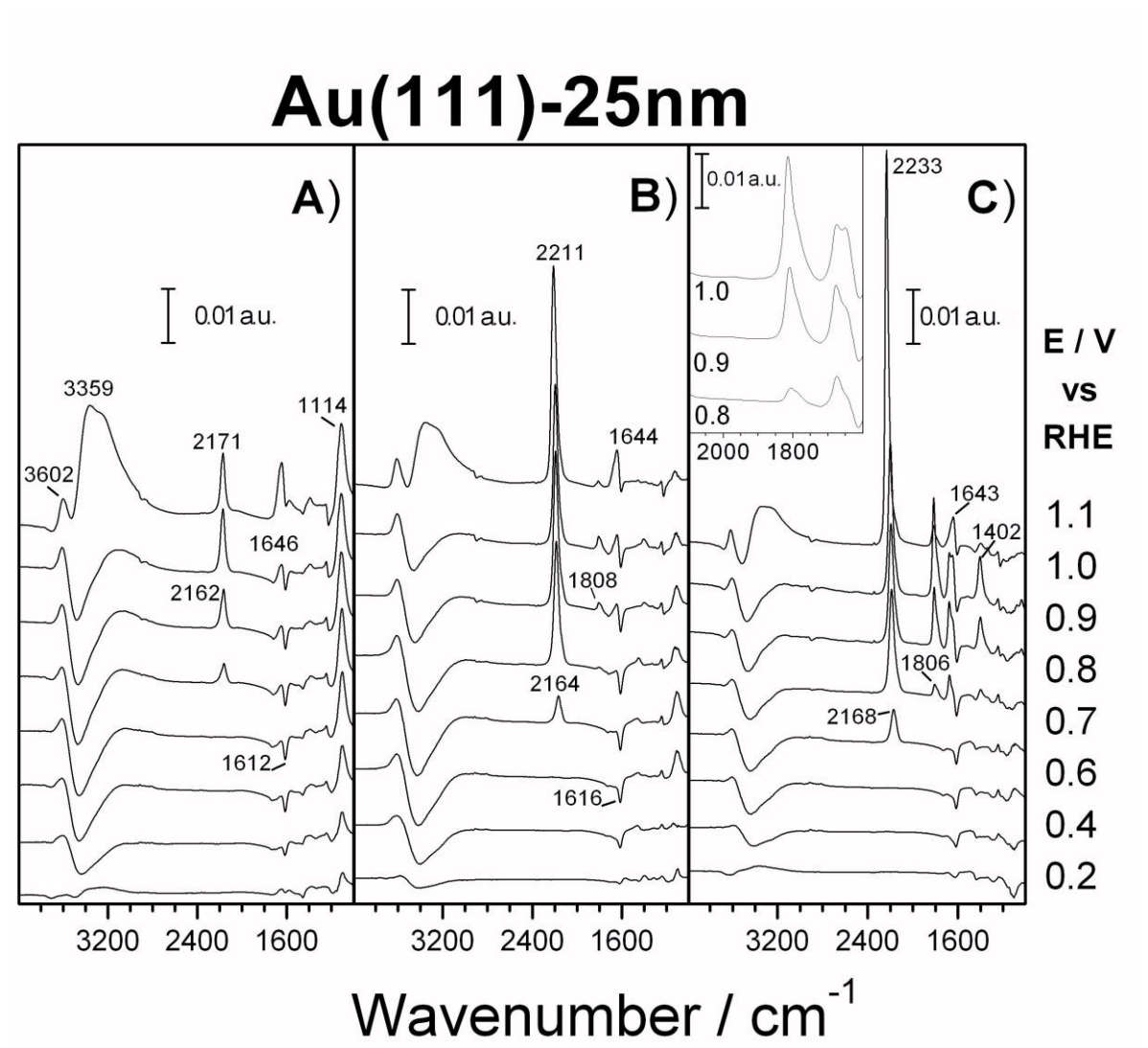

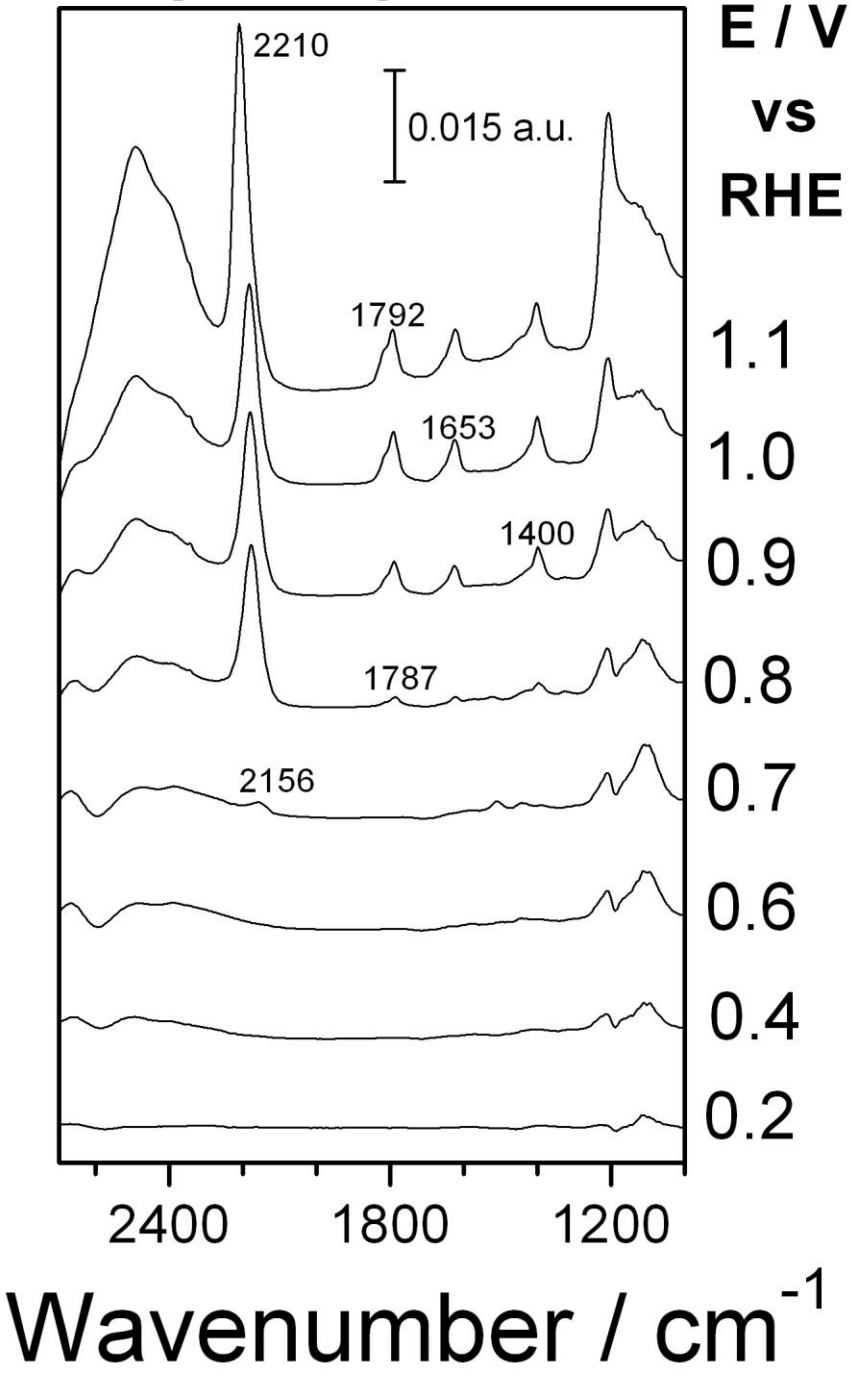

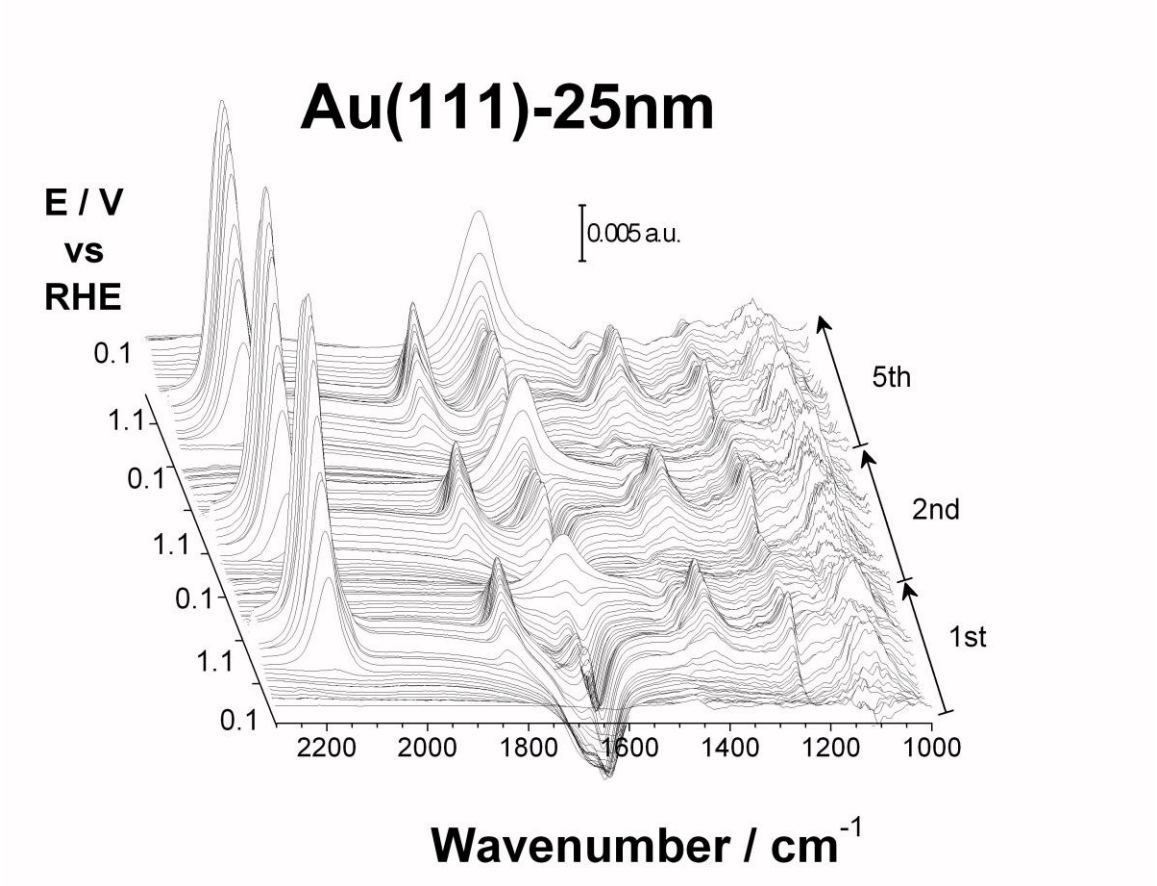

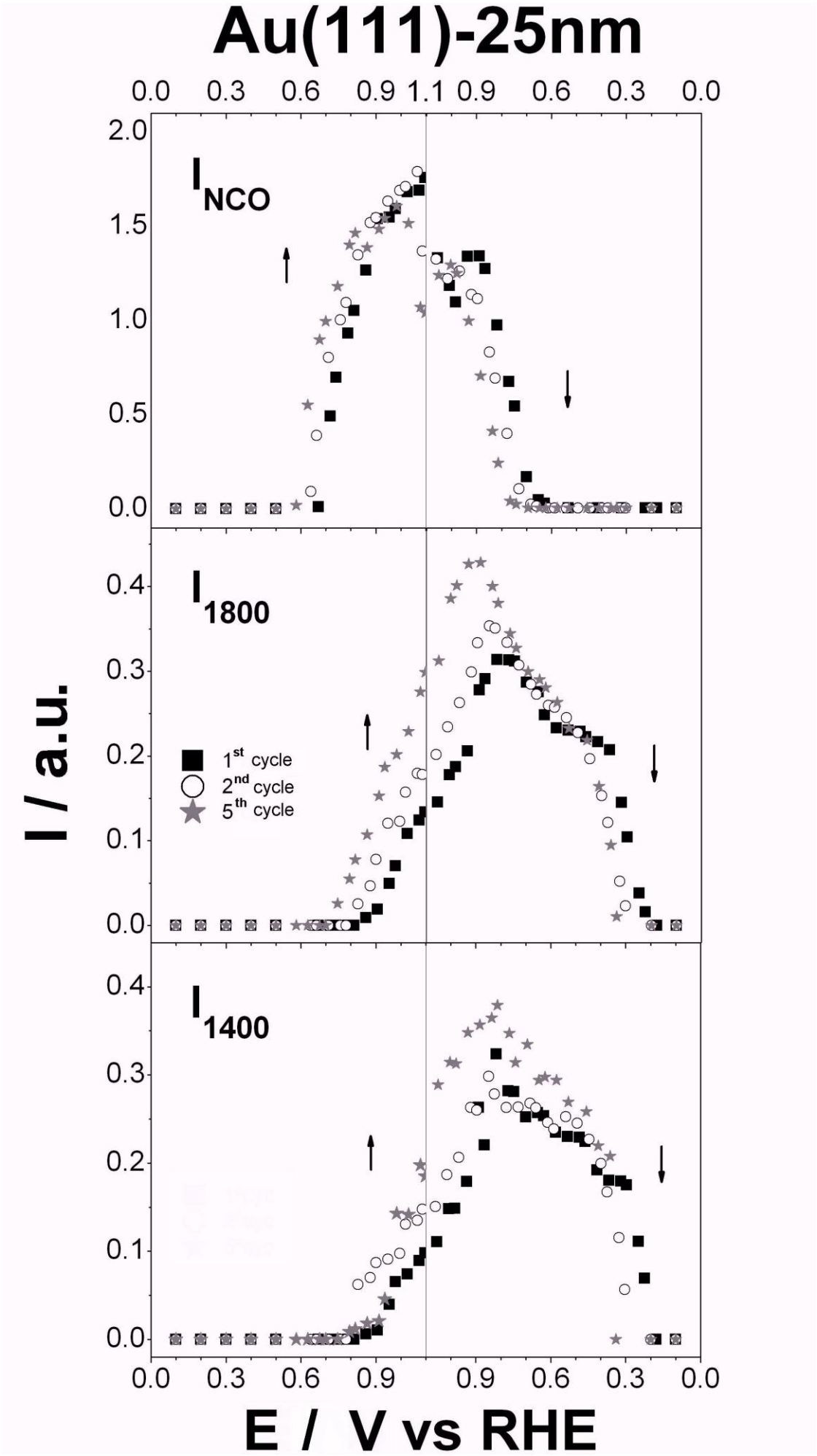

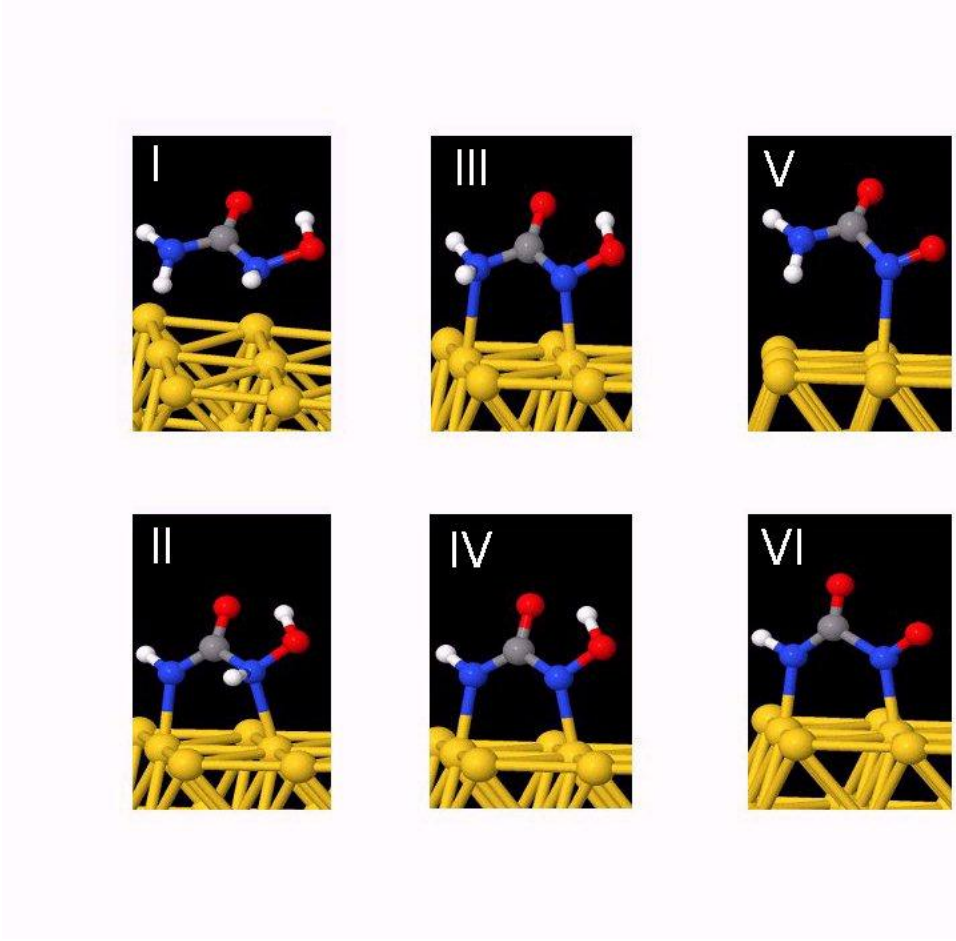

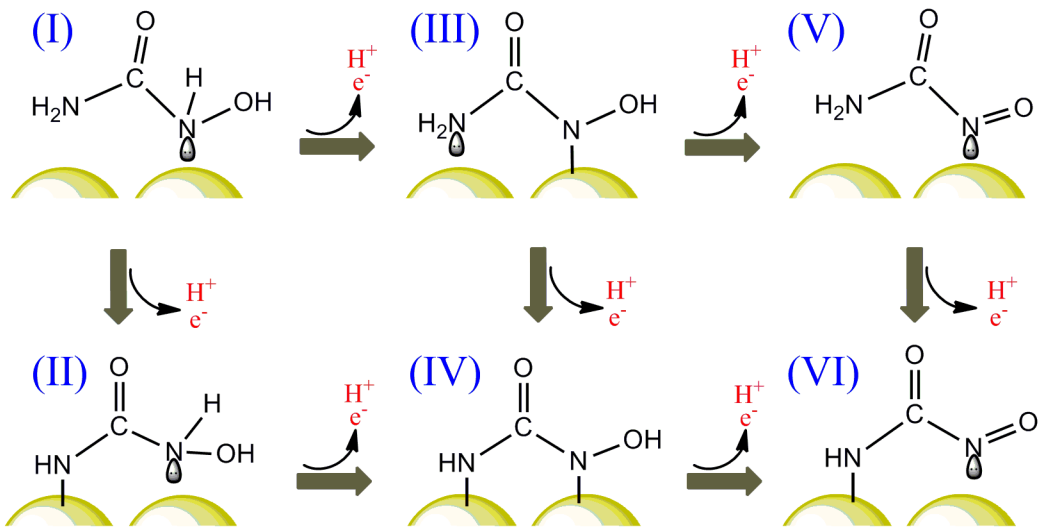

Table 1. Calculated nitrogen-gold distances (in pm) for the optimized adsorption geometries of HU and some intermediates formed by partial electrooxidation of HU. Roman numerals correspond to the structures depicted in Figure 7 and in Scheme 1.

Adspecies	**d NH_x-Au / pm**	**dN(O)-Au / pm**
I (HU)	351	299
II	219	238
III	253	224
IV	215	219
V	342	262
VI	219	223

Table 2. Experimental band frequencies measured in the ATR-SEIRA spectra (collected at 1.0 V in the 10 mM HU solution) and calculated harmonic vibrational frequencies for HU and some of its oxidation intermediates adsorbed on a model Au(111) surface (all in the range between 1900 and 1150 cm^{-1}). The calculated main contributions to the corresponding normal modes are indicated. All wavenumbers in cm^{-1}. Values in brackets correspond to the fully deuterated compound. Roman numerals correspond to the structures depicted in Figure 7 and in Scheme 1.

Experimental	Calculated					
	I	II	III	IV	V	VI
1812 (1789)	1712 (1688) νCO	1684 (1661) νCO	1620 (1592) νCO + sciss NH_2	1650 (1595) νCO + δNOH	1810 (1806) νCO	1792 (1791) νCO
1673/1650 (1623)	1572 (1355) Sciss NH_2	1464 (1260) δNOH + δCNH	1552 (1242) Sciss NH_2	1336 (1223) δNOH	1591 (1578) νNO + Sciss NH_2	1620 (1619) νNO
1403 (1400)	1498 (1178) δCNH + δNOH	1320 (1120) δCNH + δNOH	1412 (1151) δNOH	1266 (1106) Asym νNCN + δCNH	1552 (1277) Sciss NH_2 + νNO	1224 (1176) δCNH
	1375 (1121) Asym νNCN	1290 (1023) Asym νNCN + δCNH	1263 (1093) Asym νNCN	1186 (1091) δCNH	1219 (1065) Asym νNCN	1178 (950) Asym νNCN
	1310 (1058) Asym νNCN + δCNH + δNOH	1214 (1001) δCNH + Asym νNCN + νCO				